

# Study of optical transmittance of photocatalytic titanium dioxide films deposited by radiofrequency magnetron sputtering

## Estudo da transmitância óptica dos filmes de dióxido de titânio fotocatalítico depositados por “*magnetron sputtering*” usando radiofrequência

Pérciles Lopes Sant’Ana<sup>1</sup>, José Roberto Ribeiro Bortoleto<sup>1</sup>, Nilson Cristino da Cruz<sup>1</sup>, Elidiane Cipriano Rangel<sup>1</sup>, Steven Frederick Durrant<sup>1</sup>, Sofia Azevedo<sup>2</sup>, Carina Isabel S. Simões<sup>2</sup>, Vasco Teixeira<sup>2</sup>

### ABSTRACT

The optical transmittance of titanium oxide ( $\text{TiO}_2$ ) films in the ultraviolet-visible region were studied in this work. Such films have possible application in photocatalysis at room temperature. Among many candidates for photocatalysts,  $\text{TiO}_2$  is practically the only material suitable for industrial use at present. This is because  $\text{TiO}_2$  has the most efficient photocatalysis, the highest stability and the lowest cost. Photochemical reactions include the photoinduced redox reactions of adsorbed substances, or the photoinduced hydrophilic conversion of  $\text{TiO}_2$  itself. Polyethylene terephthalate (PET) was chosen as the substrate because of its flexibility, high transmission in visible light and low cost. Glass blades were used as substrates for  $\text{TiO}_2$  films for analysis by optical transmittance spectroscopy. The experimental results show that the  $\text{TiO}_2$  films deposited on glass were associated with the anatase phase with a [0 0 4] preferred orientation. Ultraviolet near infrared spectroscopy revealed the high transmittance of the films in visible light and high absorption in the ultra-violet region under most deposition conditions.

**Keywords:**  $\text{TiO}_2$ , RF sputtering, Optical properties, Photocatalysis.

### RESUMO

A transmitância óptica de filmes de dióxido de titânio ( $\text{TiO}_2$ ) na região ultravioleta-visível foi estudada neste trabalho. Tais filmes têm possível aplicação em fotocatalise à temperatura ambiente. Entre muitos candidatos a fotocatalisadores, o  $\text{TiO}_2$  é praticamente o único material adequado para uso industrial no momento. Isso ocorre porque o  $\text{TiO}_2$  possui a foto catalise mais eficiente, a maior estabilidade e o menor custo. As reações fotoquímicas incluem as reações de oxiredução fotoinduzidas de substâncias adsorvidas ou a conversão hidrofílica fotoinduzida do  $\text{TiO}_2$  em si. O tereftalato de polietileno (PET) foi escolhido como substrato devido à sua flexibilidade, alta transmissão na luz visível e baixo custo. Laminas de vidro foram utilizados como substratos para os filmes de  $\text{TiO}_2$  para análise por espectroscopia de transmitância óptica. Os resultados experimentais mostram que os filmes de  $\text{TiO}_2$  depositados no vidro foram associados à fase anatase com uma orientação preferencial em [0 0 4]. A espectroscopia de absorção no infravermelho revelou alta transmitância dos filmes sob luz visível e alta absorção na região ultravioleta sob a maioria das condições de deposição.

**Palavras-chave:**  $\text{TiO}_2$ , RF “*sputtering*”, Propriedades ópticas, fotocatalise.

1.Universidade Estadual Paulista – Câmpus Experimental de Sorocaba – Laboratório de Plasmas Tecnológicos – Sorocaba (SP), Brazil.

2.Universidade do Minho – Departamento de Física – Laboratório de Filmes Finos para a Electrónica – Braga, Portugal.

\*Correspondence author: drsantanapl@gmail.com

Received: 19 Mar 2020 Approved: 2 Apr 2020

## INTRODUCTION

Titanium dioxide ( $\text{TiO}_2$ ) is an attractive material because of its outstanding physical and chemical properties<sup>1,2</sup>. Various methods of  $\text{TiO}_2$  film deposition have recently been investigated, including pulsed laser deposition (PLD)<sup>3</sup>, atmospheric dielectric barrier discharge<sup>4,6</sup> and plasma enhanced chemical vapor deposition (PECVD)<sup>7,8</sup>.

Although PECVD has many advantages, such as high purity and the easy control of reaction parameters<sup>9</sup>, it is usually performed in high-vacuum environments or requires high temperatures for which the installation costs and the energy requirements are high. The optimal vacuum system parameters for obtaining titanium oxide thin films have been studied since 1972<sup>10</sup>. The use of sputtering technique to deposit photocatalytic thin films has been reported<sup>11</sup>. Among the various semiconductors employed,  $\text{TiO}_2$  is the most preferred material for the photocatalytic process<sup>12</sup>.

Recent studies reveal excellent  $\text{TiO}_2$  photocatalytic stability<sup>13</sup>. Another advantage is obtained when  $\text{TiO}_2$  films present high crystallinity, which influences the charge carrier lifetime, and improves photocatalytic activity<sup>14</sup>. The performance of these films in such technologies strongly depends on the  $\text{TiO}_2$  polymorphic phase employed: rutile, anatase or brookite. Anatase exhibits advantages over rutile for catalysis, photocatalysis and solar cell applications<sup>15</sup>. Some authors considered reactive magnetron sputtering as the technique to obtain  $\text{TiO}_2$  anatase<sup>16</sup>. It has been reported that the preferential growth in anatase is [001] based on Bragg-Brentano XRD analyses<sup>17,18</sup>. Moreover, the ability to control texture and the crystallinity of the  $\text{TiO}_2$  films allows increased catalytic processes<sup>19,20</sup>. Other authors report that the modification of surface morphology of semiconductor photocatalysts can give rise to a more efficient form for photocatalytic applications<sup>21</sup>.

In addition, photocatalysis with titanium dioxide ( $\text{TiO}_2$ ) using natural solar radiation is one of the most efficient processes for inactivation of bacteria including *E. coli*, *E. faecalis*, *Legionella*, etc. and some specific fungi (*Fusarium* sp.) in water<sup>22,23</sup>. Titanium dioxide is still useful as an active material in various applications such as dye-sensitized solar cells<sup>24</sup>, fuel cells and optical coatings<sup>25</sup> water purification<sup>26</sup>. Moreover,  $\text{TiO}_2$  is used to degrade organic and inorganic pollutants<sup>27,28</sup> to produce antireflection layers on low-emissivity coatings and protective layers<sup>29</sup>.

Titanium dioxide has gained attention owing to its nontoxic, chemical and environmental consistency and interesting optical properties, including its brightness and refractive index in visible region<sup>30</sup>. In addition,  $\text{TiO}_2$  of high transparency has been deposited in  $\text{Ar}/\text{O}_2$  plasmas<sup>31</sup>. Recent studies have reported the radiofrequency (RF) sputter deposition of  $\text{TiO}_2$  using  $\text{Ar}/\text{O}_2$  plasmas<sup>32</sup>.

## MATERIAL AND METHODS

### Preparation of $\text{TiO}_2$ film

The  $\text{TiO}_2$  thin films were deposited on both glass (dimensions of  $75 \times 25 \times 1$  mm)<sup>33</sup> and polyethylene terephthalate (PET) substrates of  $0.05 \times 25 \times 15$  mm, in the direct current (DC) magnetron sputtering system schematized in Fig. 1. The target was titanium of 99.9% purity and total surface area (TA) of 7854 mm<sup>2</sup>. The distance between target and substrate was 60 mm.

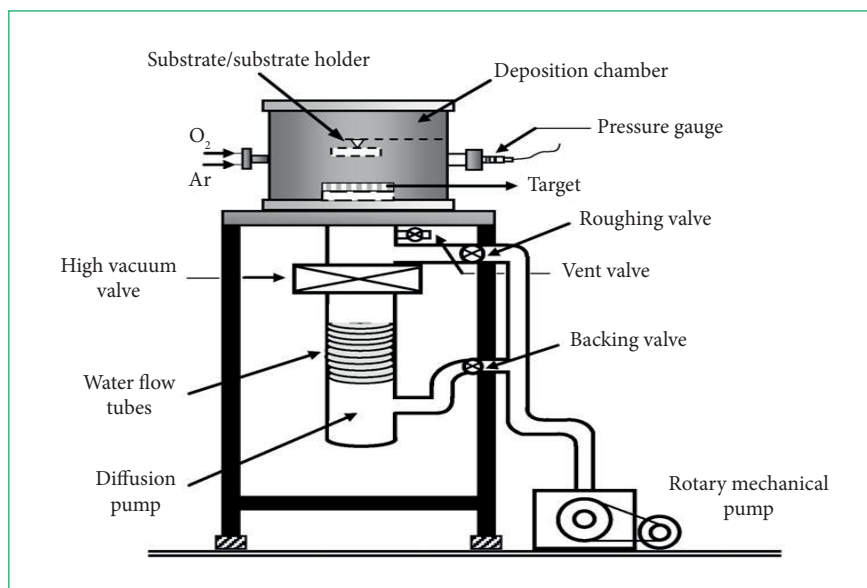


**Figure 1:** Schematic of the reactive magnetron sputtering film deposition system.

After the chamber was evacuated to a base pressure lower than  $1 \times 10^{-3}$  Pa, 50 SCCM of pure argon sputtering gas was fed to the chamber, and the discharge begun at a constant current of 0.45 A. After the discharge voltage has stabilized, 99.95% pure oxygen gas was introduced into the chamber at a constant flow rate of 10 SCCM for a deposition time of 3600 s. Working at a constant argon flow rate and discharge current, the discharge voltage increased from zero up to the threshold (applying three values of oxygen flow rate: 20, 25 or 30%), indicating that the effective reduction in the area of the metal being sputtered caused the formation of oxide. After that, the target voltage decreased to a stable value corresponding to the compound sputtering mode in which transparent  $\text{TiO}_2$  films were deposited on the substrates. Low temperature growth of anatase has been reported by a few groups using metallic Ti as a sputtering target<sup>34</sup>.

### Photocatalytic activity

Photocatalytic efficiency of  $\text{TiO}_2$  is expected to be low under visible light irradiation because UV light is about < 10% of the overall solar intensity. Thus, increasing the visible light absorption of  $\text{TiO}_2$  materials may improve the photocatalytic activity by decreasing the energy bandgap or preventing ( $e^- / h^+$ ) pair recombination by electron-hole tapping. In this study, the effects of argon and oxygen in the gas feed for  $\text{TiO}_2$  growth on the microstructure, light absorption and photocatalytic properties of  $\text{TiO}_2$  thin films were examined.

According to the literature, a satisfactory catalytic activity is seen when the films have the two phases, with the concomitant increase in the ionic radius of the grains that form the anatase phase. However, in 1995, Linsebigler *et al.* reported anatase  $\text{TiO}_2$  crystals with a gap  $\sim 3.2$  eV at  $\lambda = 387$  nm<sup>35</sup>. The same value of bandgap for anatase  $\text{TiO}_2$  (3.2 eV) was reported in previous studies<sup>36,37</sup>. Most proteins can absorb radiation of  $\lambda$  near 280 nm because of the presence of tyrosine phenylalanine, aromatic compounds and conjugated double bonds in benzene ring. These absorptions are observed in the presence of double bonds ( $\pi$ ) with transitions  $\pi$  to  $\pi^*$ , since  $n \rightarrow \pi^*$  transitions are prohibited by the selection rules. It is believed that the degree of unsaturation given by bonds of the  $\pi$  type correspond to reduced transmittance compared to  $\pi$  type connections. The influence of unsaturation on the formation of biofilms is difficult to predict<sup>38</sup>.

The electrical current and voltage parameters were also varied to seek the best deposition condition and, it can be controlled by the treatment time (deposition). Chemical reactions observed in this process were caused by the photoexcitation mechanism involving the formation of electron-hole pairs and valences. Those reactions can be seen in Fig. 2.

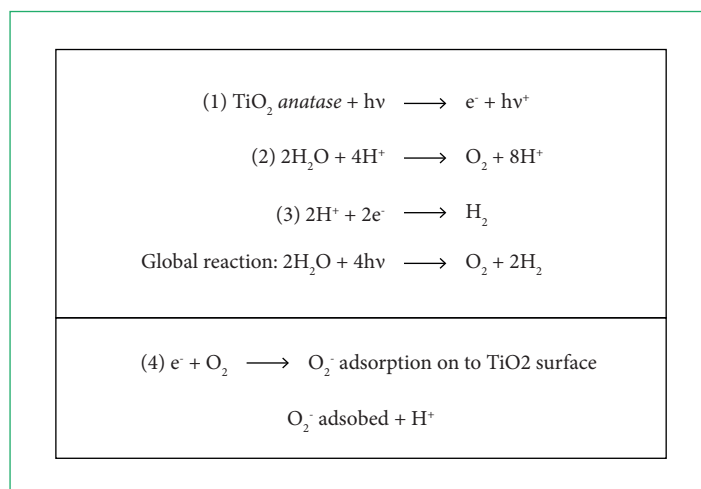


**Figure 2:** Chemical reactions stimulated by the interaction of a visible light photon with  $\text{TiO}_2$  deposited on substrates.

There are two types of photochemical reaction proceeding on the  $\text{TiO}_2$  surface when irradiated with ultraviolet light. One is photo-induced redox reactions of the adsorbed substances through “electron-hole” pairs<sup>39</sup>, and the other is hydrophilic photoinduced conversion of the film itself. Titanium dioxide is one of the most powerful oxidants because of the high oxidizing potential of holes in the valence band formed by photoexcitation<sup>40,42</sup>.

In the absence of a catalytically active substance, the oxidation process of most hydrocarbons proceeds rather slowly. A photocatalyst should decrease the activation energy of a given reaction. A heterogeneous photocatalytic system consists of semiconductor particles (photocatalyst) which are in close contact with a liquid reaction medium. By exposing the catalyst to light, excited states are generated, which are able to initiate subsequent processes, such as redox reactions and molecular changes. Owing to their electronic structure, which is characterized by a filled valence band (VB) and an empty conduction band (CB), metal oxides, such as  $\text{TiO}_2$ , can act as sensitizers for light-induced redox processes. For example, UV light can excite pairs of electrons and holes; an electron ( $e^-_{\text{CB}}$ ) is promoted to the conduction band while a positive hole ( $h^+_{\text{VB}}$ ) is generated in the valence band. The photo-generated electrons then react with molecular

oxygen ( $O_2$ ) to produce super-oxide radical anions ( $O_2^-$ ), and the photo-generated holes react with water to produce hydroxyl ( $OH^\cdot$ ) radicals. These two types of reactive radicals can work together to decompose organic compounds.

### Characterization and conditions

A Shimadzu UV-310PC scanning spectrophotometer was used to measure the transmittance spectrum of  $TiO_2$  films as a function in the wavelength range from 200 to 900 nm. This procedure is highly reproducible, and no error-bar was generated. Table 1 shows the parameters adopted for these series of depositions. The temperature determined by the plasma kinetics ranged from 40 and 45 °C.

**Table 1:** Initial conditions for  $TiO_2$  deposition, described by the code #A (Ar and O proportion).

Experimental parameters	#A1 Ar = 20% (50 SCCM) O <sub>2</sub> = 25% (10 SCCM)	#A2 Ar = 20% (50 SCCM) O <sub>2</sub> = 25% (10 SCCM)	#A3 Ar = 20% (50 SCCM) O <sub>2</sub> = 30% (10 SCCM)	#A4 Ar = 35% (50 SCCM) O <sub>2</sub> = 20% (10 SCCM)	#A5 Ar = 35% (50 SCCM) O <sub>2</sub> = 20% (10 SCCM)	#A6 Ar = 45% (50 SCCM) O <sub>2</sub> = 20% (10 SCCM)
Electric current (A)	0.45	0.45	0.45	0.2	0.2	0.2
Voltage (V)	519	517	507	437	437	416
RF power (W)	233	232	228	87	87	83
Deposition time (s)	3600	3600	3600	3600	3600	3600
Background pressure (mbar)	$6.3 \times 10^{-3}$	$6.4 \times 10^{-3}$	$5.7 \times 10^{-3}$	$9.2 \times 10^{-3}$	$9.2 \times 10^{-3}$	$1.26 \times 10^{-3}$

In addition, Table 2 shows the different sample positions on the electrode for the deposition of  $TiO_2$  films.

**Table 2:** Sample positions on the electrode for the second series of experiments identified by #B1 to #B6.

Code	Placement/assignment
#B1	Glass in the center of the electrode holder associated with the condition #A5
#B2	Glass in the electrode holder edge associated with the condition #A5
#B3	Glass in the center of the electrode holder associated with the condition #A6
#B4	Glass in the electrode holder edge associated with the condition #A6
#B5	PET in the electrode holder edge associated with the condition #A5
#B6	PET in the center of the electrode holder associated with the condition #A5

## RESULTS

### Crystallographic directions, composition of $TiO_2$ films

The  $TiO_2$  films deposited under these conditions were studied using X-ray diffraction (XRD) and X-ray photoelectron spectroscopy (XPS). For some applications such as transparent conductors, the anatase phase with its larger crystallite size is preferable to obtain electrons mobilities. The average crystallite sizes for the  $TiO_2$  films can be calculated from the broadening of the diffraction peak using Scherrer's formula,  $D = 0.9\lambda/B \cos\theta$ , where  $\lambda$  is the wavelength of Cu  $K_\alpha$  radiation,  $B$  is the full width at half maximum (FWHM) of XRD peaks and  $\theta$  the Bragg diffraction angle of the line<sup>43</sup>. At  $T_{\text{substrate}} \geq 200$  °C, the films tend to have random crystallite orientation and exhibit (0 0 4) and (2 0 0) reflections of the anatase phase, indicating that the growth temperature has a great impact on the structural properties of the prepared  $TiO_2$  films<sup>44</sup>.

The O1s XPS spectrum of  $TiO_2$  films deposited in Ar-O plasmas was studied. The presence of an asymmetric component at the higher binding energy (BE) side with respect to the main peak (OI) indicates the existence of different chemical states of oxygen. The peak is deconvoluted into two components: the first at lower BE (530.64 eV) can be ascribed to the O1s core peak of O2- bound to Ti4+ in  $TiO_2$ <sup>45</sup>, whereas the higher BE component located at 531.82 eV, may arise from the contribution of oxygen to Ti-OH bonds<sup>46</sup>. The other component (OII) at the higher BE of 532.62 eV is associated with adsorbed molecular bonds such as C=O, O-C-O or O=C-O<sup>47</sup>. Carbon probably was ejected from PET by sputtering and etching reactions, linking with oxygen introduced in vacuum chamber.

### Optical transmittance in the UV-visible region

Titanium oxide films are transparent in the visible region and their transparency shows a sharp decrease in the UV region. For the initial studied samples, Fig. 3 shows the transmittance curves  $T(\lambda)$  as a function of wavelength for different proportions of argon and

oxygen gases, while Fig. 4 shows the results for different positions of the substrates on the upper electrode. The spectra were acquired immediately after removal of the samples from the reactor (also, immediately after deposition). Ultraviolet photons excite electrons from the valence band (vb) to conduction band (cb), leading to two types of charge carriers, electrons ( $e^-$ ) and holes ( $h^+$ ). These carriers are responsible for the activation of chemical reactions<sup>48,49</sup>.

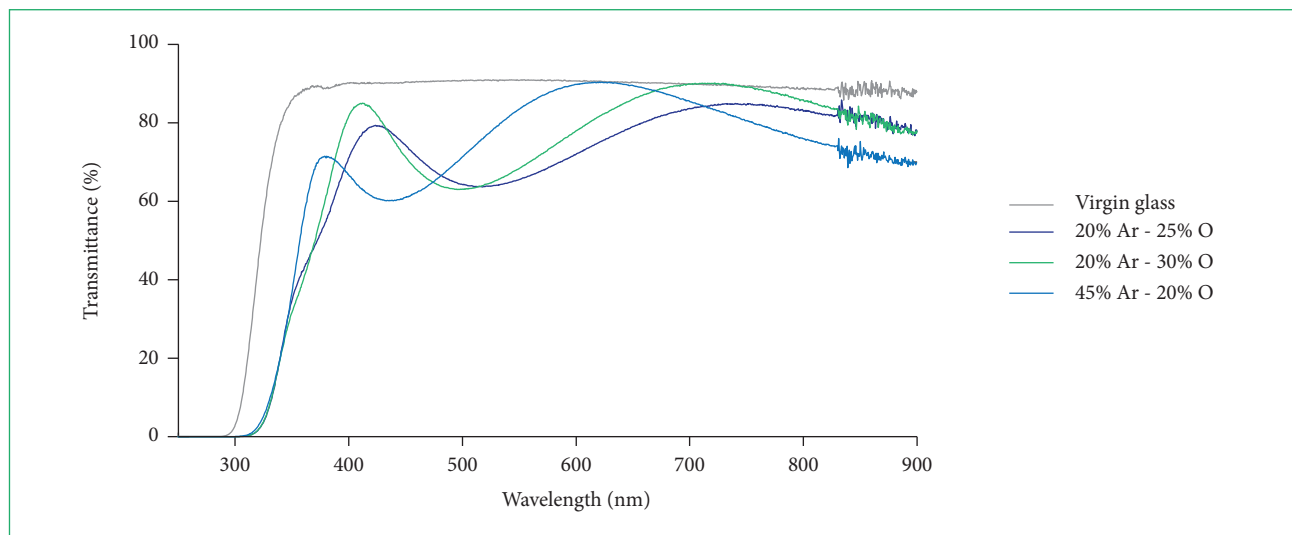


**Figure 3:** Optical transmittance as a function of wavelength ( $\lambda$ ) in the visible region, measured on the  $\text{TiO}_2$  deposited on glass by RF magnetron sputtering. The flow rates of argon and oxygen were 10 and 50 SCCM, respectively, for a deposition time of 3600 s.

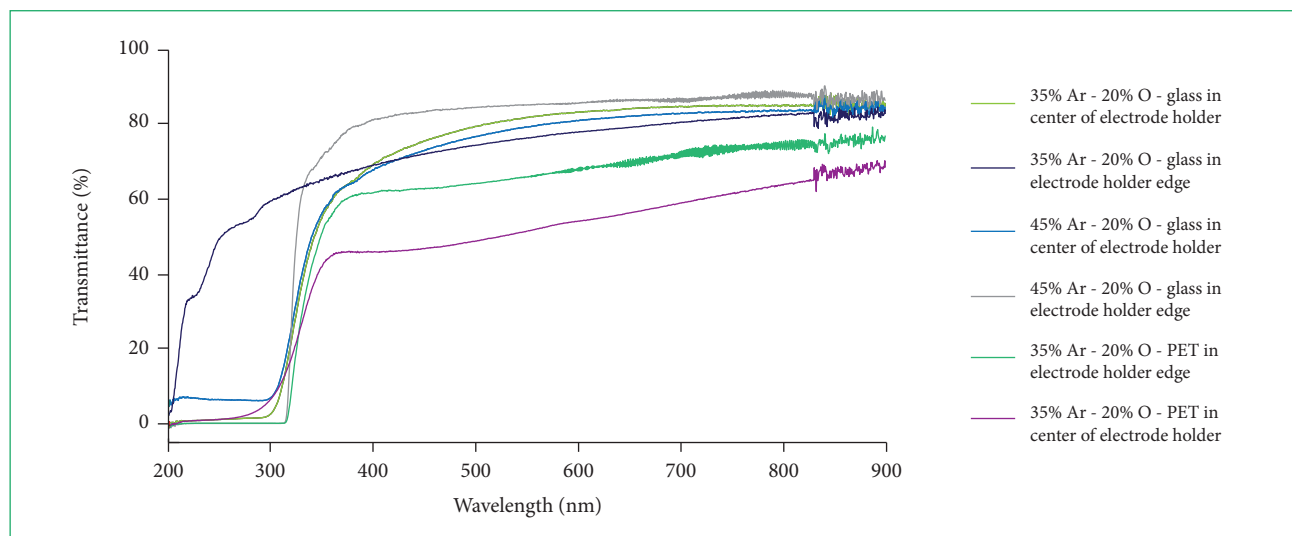


**Figure 4:** Optical transmittance as a function of wavelength in the visible of  $\text{TiO}_2$  deposited onto glass substrates by RF magnetron sputtering. The flow rates of argon and oxygen were 10 and 50 SCCM, respectively, for a deposition time of 3600 s.

A sharp decrease in the  $T(\lambda)$  curves in the visible region was seen for all gas proportions shown in Fig. 3 and, except under condition B3, also seen in Fig. 4. This implies that a polymer packing with this film in most of conditions, when exposed to ambient light may have on its surface an antimicrobial activity stimulated by photocatalysis caused by UV light through films, since absorption occurs in the visible region, including the blue ultraviolet radiation. Harmful bacteria may be destroyed when exposed to radiation of  $\lambda$  between 190 and 250 nm. The bactericide action of  $\text{TiO}_2$  arises from the existence of reactive groups, such as hydroxyl, on its surface. Reactive species, such as  $\text{-OH}$  and  $\text{O}^{2-}$ , decompose organic compounds. This mechanism is responsible for the antibacterial action of irradiated  $\text{TiO}_2$  surfaces<sup>50</sup>. Ultraviolet irradiation of  $\text{TiO}_2$  promotes electrons ( $e^-$ ) from the valence band to the conduction band, which leaves positive charge carrier holes ( $h^+$ ) in the valence band. The  $e^-$  and  $h^+$  charges migrate in random directions to the bulk or the surface. Those elementary charges that reach the surface of the catalyst can react with electron-donor and electron-acceptor species present at the semiconductor/electrolyte interface<sup>51</sup>. Moreover, the high absorption below 200 nm is associated with crystal-field splitting. It is known that Ti has octahedral coordination in anatase  $\text{TiO}_2$  causing a crystal-field splitting of the d-orbitals of titanium into two subbands: the

eg and the t<sub>2g</sub> orbitals<sup>52</sup>; the eg orbitals (dz<sup>2</sup> and dx<sup>2</sup>-y<sup>2</sup>) which point directly toward the oxygen ligands and form r-type orbitals; the t<sub>2g</sub> orbitals (dxy, dyz and dxz) point between the oxygen neighbors and form p-orbitals. The repulsive force between the dxy, dyz, dxz and oxygen ligands is weaker leading to a decreased energy for those orbitals. The Ti(3d4s4p) orbitals are then linearly combined with the O(2s2p) orbitals to form the molecular orbitals. Previous studies revealed that the upper t<sub>2g</sub><sup>\*</sup> and e<sub>g</sub><sup>\*</sup> are mainly of Ti3d character and form the conduction band, and the lower t<sub>2g</sub> and e<sub>g</sub> are mainly of O2p character and form the valence band<sup>53,54</sup>.

## DISCUSSION

In recent decades, TiO<sub>2</sub> semiconductors have attracted great interest due to their low cost and low toxicity, together with their high transparency, high refractive index, and good chemical stability. Nowadays, TiO<sub>2</sub> thin films are used for a variety of applications, ranging from selective absorbing coatings to photovoltaic solar cells, gas sensors and photocatalysis. The literature reports the use of TiO<sub>2</sub> films in advanced oxidative processes (POA), mainly in heterogeneous photocatalysis<sup>55</sup>. The use of thin films of TiO<sub>2</sub> in heterogeneous photocatalysis is possible because of its semiconducting characteristics, since it is active under irradiations for 300 nm < λ < 390 nm and remains stable after many catalytic cycles<sup>56</sup>, owing to its large bandgap (3.2 eV)<sup>57-59</sup>. Semiconductor photocatalysis is one of the most promising processes for purification of water<sup>60,61</sup>. Some studies point out that anatase TiO<sub>2</sub> has more efficient photocatalytic properties<sup>62</sup>. Moreover, some studies report that the addition of H<sub>2</sub>O<sub>2</sub> as a photocatalytic activity accelerator has also been evaluated under natural sunlight. A weight relation of 1:2 of TiO<sub>2</sub> to H<sub>2</sub>O<sub>2</sub> was tested<sup>63</sup>, using the TiO<sub>2</sub> concentration that gave the fastest inactivation, i.e. 35 mg L<sup>-1</sup> of TiO<sub>2</sub>. On the other hand, samples with only TiO<sub>2</sub> were more efficient for the inactivation of *Cryptosporidium parvum* in water under simulated and natural solar radiation. A complete account of the mechanism of bacterial inactivation has been reported in some recent reviews<sup>64</sup>. The preparation of TiO<sub>2</sub> thin films by sputtering has prominent advantages such as clean process (without intermediate chemical products), high reproducibility and easy scale-up to produce uniform films on large area substrates. Different sputtering processes have been used for TiO<sub>2</sub> deposition, in RF or DC modes<sup>65</sup>. In the case of TiO<sub>2</sub>/solar radiation, the inhibition of the process may be caused by the effect of clogging the catalyst surface by organic molecules or microorganisms already present in this type of water. Therefore, competition occurs for the holes generated on the surface of the TiO<sub>2</sub>. When H<sub>2</sub>O<sub>2</sub> is added to TiO<sub>2</sub>, an enhancement occurs because of the already described process of inhibition of electron/hole recombination is reduced and therefore generates more HO•<sup>66</sup>. When a semiconductor is excited with sunlight, absorption of photons with energy higher than the band gap leads to the creation of electron-hole pairs. These photoexcited charge carriers react with the adsorbed oxygen molecules and water molecules leading to the formation of superoxide radicals (•O<sub>2</sub><sup>-</sup>) and hydroxyl (•OH) radicals, respectively. These reactive oxygen species interact with the adsorbed toxic pollutants resulting in their degradation<sup>67-69</sup>. Thus, the authors of this work strongly recommend growing films under the conditions given by this work for photocatalysis, and the optical spectra confirm the suggested applications, since they presented high transmittance in the visible region, up to 350 nm, and high absorption near to and below 300 nm, which stimulates photocatalytic activity. About degradative processes on substrates: It is characteristic for UV degradative processes to occur under oxygen starvation and diminished UV beam penetration across the material thickness. Oxygen diffusion-limited reaction is caused when the oxygen from the atmosphere is consumed by rapid reaction near the illuminated surface before it can diffuse into the interior to react there<sup>70</sup>. It is quite common in photooxidation of polymers. Oxygen starvation depends on the diffusion coefficient for oxygen in a particular polymer. It is, for example, two orders of magnitude smaller for PET than for polyethylene<sup>70</sup>. The PET samples used in this work did not present any signal of degradation, due to UV radiation generated by the plasma deposition. Anyway, it is suggested to study the mechanisms of photodegradation of PET under UV for future studies, whose conditions can be found in Fechine *et al.*<sup>71,72</sup>.

## CONCLUSION

Radiofrequency magnetron sputtering is an excellent technique to grow anatase TiO<sub>2</sub> films for photocatalysis reactions. The material produced is suitable for some important applications such as water treatment, pollutant treatment, self-cleaning surfaces, so on. The spectra reveal good deposition conditions for all argon/oxygen proportions, since the curves were dislocated in relation to those of glass substrates, yielding high transmittance in the visible, up to 350 nm, and high absorption near to and below 300 nm, which stimulates photocatalytic activity. In relation to the spectrum as a function of the sample position on the electrodes, only condition #B2 (glass in the electrode edge) did not result in high absorption in the visible region. At the electrode edge, there is no linear electric field, and the film does not grow. The best condition (#A5, #B1) produced high transmittance for longer wavelengths in the visible (up to 350 nm), high absorption for lower wavelengths in the visible to UV-visible, with low surface roughness (~5 nm).



## FUNDING

Conselho Nacional de Desenvolvimento Científico e Tecnológico [<https://doi.org/10.13039/501100003593>]

Fundação de Amparo à Pesquisa do Estado de São Paulo [<https://doi.org/10.13039/501100001807>]

#Project 2017/15853-0

## REFERENCES

1. Abdin Z, Alim MA, Saidur R, Islam MR, Rashmi W, Mekhilef S, et al. Solar energy harvesting with the application of nanotechnology. *Renew Sust Energ Rev.* 2013;26:837-52. <https://doi.org/10.1016/j.rser.2013.06.023>
2. Maçaira J, Andrade L, Mendes A. Review on nanostructured photoelectrodes for next generation dye-sensitized solar cells. *Renew Sust Energ Rev.* 2013;27:334-49. <https://doi.org/10.1016/j.rser.2013.07.011>
3. Henkel B, Neubert T, Zabel S, Lamprecht C, Selhuber-Unkel C, Rätzke K, et al. Photocatalytic properties of titania thin films prepared by sputtering versus evaporation and aging of induced oxygen vacancy defects. *Appl Catal B Environ.* 2016;180:362-71. <https://doi.org/10.1016/j.apcatb.2015.06.041>
4. Ananth A, Gandhi MS, Mok YS. A dielectric barrier discharge (DBD) plasma reactor: an efficient tool to prepare novel RuO<sub>2</sub> nanorods. *J Phys D: Appl Phys.* 2013;46(15):155202. <https://doi.org/10.1088/0022-3727/46/15/155202>
5. Wang D, Yang Q, Guo Y, Liu X, Shi J, Zhang J. One step growth of TiO<sub>2</sub> crystal trees by atmospheric pressure plasma jet. *Mater Lett.* 2011;65(15-16):2526-9. <https://doi.org/10.1016/j.matlet.2011.05.054>
6. Zille A, Fernandes MM, Francesco A, Tzanov T, Fernandes M, Oliveira FR, et al. Size and aging effects on antimicrobial efficiency of silver nanoparticles coated on polyamide fabrics activated by atmospheric DBD plasma. *ACS Appl Mater Interfaces.* 2015;7(25):13731-44. <https://doi.org/10.1021/acsami.5b04340>
7. Ostrikov KK, Seo DH, Mehdi-pour H, Cheng Q, Kumar S. Plasma effects in semiconducting nanowire growth. *Nanoscale.* 2012;4(5):1497-1508. <https://doi.org/10.1039/C1NR10658A>
8. Attri P, Arora B, Choi EH. Retraction: Utility of plasma: a new road from physics to chemistry. *RSC Adv.* 2013;3:12540-67. Erratum in: *RSC Adv.* 2017;7:15735. <https://doi.org/10.1039/C7RA90034A>
9. Li ML, Huang GS, Wang DX, Zhang J, Shi JJ, Mei YF. Atmospheric growth and strong visible luminescence of anatase titanium oxide films with various orientations. *J Mater Chem A.* 2014;2(19):6708-13. <https://doi.org/10.1039/C4TA00730A>
10. Mardare D, Tasca M, Delibas M, Rusu GI. On the structural properties and optical transmittance of TiO<sub>2</sub> r.f. sputtered thin films. *Appl Surf Sci.* 2000;156(1-4):200-6. [https://doi.org/10.1016/S0169-4332\(99\)00508-5](https://doi.org/10.1016/S0169-4332(99)00508-5)
11. Thongsuriwong K, Amornpitoksuk P, Suwanboon S. Structure, morphology, photocatalytic and antibacterial activities of ZnO thin films prepared by sol-gel dip-coating method. *Adv Powder Technol.* 2013;24(1):275-80. <https://doi.org/10.1016/j.appt.2012.07.002>
12. Ken-Ichi O, Yasunori Y, Hiroki T, Masashi T, Akira I. Heterogeneous photocatalytic decomposition of phenol over TiO<sub>2</sub> powder. *Bull Chem Soc Jpn.* 1985;58(7):2015-22. <https://doi.org/10.1246/bcsj.58.2015>
13. Chen Q, Liu Q, Hubert J, Huang W, Baert K, Wallaert G, et al. Deposition of photocatalytic anatase titanium dioxide films by atmospheric dielectric barrier discharge. *Surf Coat Technol.* 2017;310:173-9. <https://doi.org/10.1016/j.surfcoat.2016.12.077>
14. Marshall R. Semiconductor composites: Strategies for enhancing charge carrier separation to improve photocatalytic activity. *Adv Funct Mater.* 2014;24(17):2421-40. <https://doi.org/10.1002/adfm.201303214>
15. Liu L, Zhao H, Andino JM, Li Y. Photocatalytic CO<sub>2</sub> reduction with H<sub>2</sub>O on TiO<sub>2</sub> nanocrystals: comparison of anatase, rutile, and brookite polymorphs and exploration of surface chemistry. *ACS Catal.* 2012;2(8):1817-28. <https://doi.org/10.1021/cs300273q>
16. Wang Z, Zeng W, Gu L, Saito M, Tsukimoto S, Ikuhara Y. Atomic-scale structure and electronic property of the LaAlO<sub>3</sub>/TiO<sub>2</sub> interface. *J Appl Phys.* 2010;108(11):113701. <https://doi.org/10.1063/1.3516496>
17. Xu H, Feng X, Luan C, Ma J. Preparation and characterization of single crystalline anatase TiO<sub>2</sub> epitaxial films on LaAlO<sub>3</sub>(001) substrates by metal organic chemical vapor deposition. *Scr Mater.* 2016;124:76-80. <https://doi.org/10.1016/j.scriptamat.2016.06.040>
18. Krupski K, Sanchez AM, Krupski A, McConville CF. Optimisation of anatase TiO<sub>2</sub> thin film growth on LaAlO<sub>3</sub>(001) using pulsed laser deposition. *Appl Surf Sci.* 2016;388(B):684-90. <https://doi.org/10.1016/j.apsusc.2016.02.214>
19. Luttrell T, Halpegamage S, Tao J, Kramer A, Sutter E, Batzill M. Why is anatase a better photocatalyst than rutile? – Model studies on epitaxial TiO<sub>2</sub> films. *Sci Rep.* 2014;4:4043. <https://doi.org/10.1038/srep04043>
20. Wu HB, Chen JS, Hng HH, Lou XWD. Nanostructured metal oxide-based materials as advanced anodes for lithium-ion batteries. *Nanoscale.* 2012;4(8):2526-42. <https://doi.org/10.1039/c2nr11966h>
21. Gaya UI. *Heterogeneous photocatalysis using inorganic semiconductor solids.* Dordrecht: Springer; 2014. <https://doi.org/10.1007/978-94-007-7775-0>

22. Polo-López MI, Castro-Alferez M, Oller I, Fernández-Ibáñez P. Assessment of solar photo-Fenton, photocatalysis, and H<sub>2</sub>O<sub>2</sub> for removal of phytopathogen fungi spores in synthetic and real effluents of urban wastewater. *Chem Eng J*. 2014;257:122-30. <https://doi.org/10.1016/j.cej.2014.07.016>
23. Rodríguez-Chueca J, Polo-López MI, Mosteo R, Ormad MP, Fernández-Ibáñez P. Disinfection of real and simulated urban wastewater effluents using a mild solar photo-Fenton. *Appl Catal B Environ*. 2014;150-151:619-29. <https://doi.org/10.1016/j.apcatb.2013.12.027>
24. Chamanzadeh Z, Noormohammadi M, Zahedifar M. Enhanced photovoltaic performance of dye sensitized solar cell using TiO<sub>2</sub> and ZnO nanoparticles on top of free standing TiO<sub>2</sub> nanotube arrays. *Mater Sci Semicond Process*. 2017;61:107-13. <https://doi.org/10.1016/j.mssp.2017.01.006>
25. Mazur M, Wojcieszak D, Kaczmarek D, Domaradzki J, Song S, Gibson D, et al. Functional photocatalytically active and scratch resistant antireflective coating based on TiO<sub>2</sub> and SiO<sub>2</sub>. *Appl Surf Sci*. 2016;380:165-71. <https://doi.org/10.1016/j.apsusc.2016.01.226>
26. Arcadipane E, Sanz R, Miritello M, Impellizzeri G, Grimaldi MG, Privitera V, et al. TiO<sub>2</sub> nanowires on Ti thin film for water purification. *Mater Sci Semicond Process*. 2016;42(1):24-7. <https://doi.org/10.1016/j.mssp.2015.07.055>
27. Natarajan S, Bhuvaneshwari M, Lakshmi DS, Mrudula P, Chandrasekaran N, Mukherjee A. Antibacterial and antifouling activities of chitosan/TiO<sub>2</sub>/Ag NPs nanocomposite films against packaged drinking water bacterial isolates. *Environ Sci Pollut Res Int*. 2016;23(19):19529-40. <https://doi.org/10.1007/s11356-016-7102-6>
28. Cozmuta AM, Peter A, Cozmuta LM, Nicula C, Crisan L, Baia L, et al. Active packaging system based on Ag/TiO<sub>2</sub> nanocomposite used for extending the shelf life of bread. Chemical and microbiological investigations. *Packag Technol Sci*. 2015;28(4):271-84. <https://doi.org/10.1002/pts.2103>
29. Mohamad SH, Idris MI, Abdullah HZ, Ismail AF. Short review of ultrafiltration of polymer membrane as a self-cleaning and antifouling in the wastewater system. *Adv Mat Res*. 2013;795:318-23. <https://doi.org/10.4028/www.scientific.net/AMR.795.318>
30. Xu Y, Zhang M, Zhang M, Lv J, Jiang X, He G, et al. Controllable hydrothermal synthesis, optical and photocatalytic properties of TiO<sub>2</sub> nanostructures. *Appl Surf Sci*. 2014;315:299-306. <https://doi.org/10.1016/j.apsusc.2014.07.110>
31. Tao J, Pan H, Wong LM, Wong TI, Chai JW, Pan J, et al. Mechanism of insulator-to-metal transition in heavily Nb doped anatase TiO<sub>2</sub>. *Mater Res Express*. 2014;1(1):015911. <https://doi.org/10.1088/2053-1591/1/1/015911>
32. Safeen K, Micheli V, Bartali R, Gottardi G, Safeen A, Ullah H, et al. Synthesis of conductive and transparent Nb-doped TiO<sub>2</sub> films: Role of the target material and sputtering gas composition. *Mater Sci Semicond Process*. 2017;66:74-80. <https://doi.org/10.1016/j.mssp.2017.04.012>
33. Molamohammadi M, Arman A, Achour A, Astinchap B, Ahmadpourian A, Boochani A, et al. Microstructure and optical properties of cobalt-carbon nanocomposites prepared by RF-sputtering. *J Mater Sci: Mater Electron*. 2015;26(8):5964-69. <https://doi.org/10.1007/s10854-015-3170-5>
34. Karuppasamy A, Subrahmanyam A. Studies on the room temperature growth of nanoanatase phase TiO<sub>2</sub> thin films by pulsed dc magnetron with oxygen as sputter gas. *J Appl Phys*. 2007;101(6):064318. <https://doi.org/10.1063/1.2714770>
35. Linsebigler AL, Lu G, Yates JT. Photocatalysis on TiO<sub>2</sub> surfaces: principles, mechanisms, and selected results. *Chem Rev*. 1995;95(3):735-58. <https://doi.org/10.1021/cr00035a013>
36. Castro MV, Rebouta L, Alpuim P, Cerqueira MF, Benelmekki M, Garcia CB, et al. Optimisation of surface treatments of TiO<sub>2</sub>:Nb transparent conductive coatings by a post-hot-wire annealing in a reducing H<sub>2</sub> atmosphere. *Thin Solid Films*. 2014;550:404-12. <https://doi.org/10.1016/j.tsf.2013.11.044>
37. Nair PB, Justinivictor VB, Daniel GP, Joy K, Raju KCJ, Kumar DD, et al. Optical parameters induced by phase transformation in RF magnetron sputtered TiO<sub>2</sub> nanostructured thin films. *Prog Nat Sci*. 2014;24(3):218-25. <https://doi.org/10.1016/j.pnsc.2014.05.010>
38. Sant'Ana PL. Polymers treated by plasma for optical devices and food packaging: Giving a technological ends for commercial and recycled plastics. Australia: Scholars' Press; 2018.
39. Kaneko M, Okura I. Photocatalysis: Science and Technology (Biological and Medical Physics, Biomedical Engineering). Berlin: Springer; 2002.
40. Gaya UI, Abdullah AH. Heterogeneous photocatalytic degradation of organic contaminants over titanium dioxide: A review of fundamentals, progress and problems. *J Photochem Photobiol C: Photochem. Rev*. 2008;9(1):1-12. <https://doi.org/10.1016/j.jphotochemrev.2007.12.003>
41. Hoffmann MR, Martin ST, Choi W, Bahnemann DW. Environmental Applications of Semiconductor Photocatalysis. *Chem Rev*. 1995;95(1):69-96. <https://doi.org/10.1021/cr00033a004>
42. Morrison SR. Electrochemistry at semiconductor and oxidized metal electrodes. New York: Plenum Press; 1980.
43. Cullity BD. Elements of X-ray diffraction. Michigan: Addison-Wesley Publishing Company; 1978.
44. Singh P, Kaur D. Room temperature growth of nanocrystalline anatase TiO<sub>2</sub> thin films by dc magnetron sputtering. *Physica B Condens Matter*. 2010;405(1):1258-66. <https://doi.org/10.1016/j.physb.2009.11.061>
45. Moulder JF, Stickle WF, Sobol PE, Bomben KD. Handbook of X-ray photoelectron spectroscopy: a reference book of standard spectra for identification and interpretation of Xps data. Eden Prairie: Physical Electronics; 1995.
46. Beamson G, Briggs D. High resolution monochromated X-ray photoelectron spectroscopy of organic polymers: A comparison between solid state data for organic polymers and gas phase data for small molecules. *Mol Phys*. 1992;76(4):919-36. <https://doi.org/10.1080/00268979200101761>



47. Luciu I, Bartali R, Laidani N. Influence of hydrogen addition to an Ar plasma on the structural properties of TiO<sub>2</sub>-x thin films deposited by RF sputtering. *J Phys D: Appl Phys.* 2012;45(34):345302. <https://doi.org/10.1088/0022-3727/45/34/3453>
48. Yang, L, Yu LE, Ray MB. Photocatalytic oxidation of paracetamol: dominant reactants, intermediates, and reaction mechanisms. *Environ. Sci. Technol.* 2009;43(2):460-65 <https://doi.org/10.1021/es8020099>
49. Banerjee S, Dionysiou DD, Pillai SC. Self-cleaning applications of TiO<sub>2</sub> by photo-induced hydrophilicity and photocatalysis. *Appl Catal B Environ.* 2015;176-177:396-428. <https://doi.org/10.1016/j.apcatb.2015.03.058>
50. Soethe VL, Delatorre RG, Ramos EM, Parucker ML. TiO<sub>2</sub> thin films for biofouling applications. *Mat Res.* 2017;20(Suppl 2):426-31. <https://doi.org/10.1590/1980-5373-mr-2016-1116>
51. Fujishima A, Zhang X, Tryk DA. TiO<sub>2</sub> photocatalysis and related surface phenomena. *Surf Sci Rep.* 2008;63(12):515-82. <https://doi.org/10.1016/j.surfrep.2008.10.001>
52. Diebold U. The surface science of titanium dioxide. *Surf Sci Rep.* 2003;48(5-8):53-229. [https://doi.org/10.1016/S0167-5729\(02\)00100-0](https://doi.org/10.1016/S0167-5729(02)00100-0)
53. Yu J, Zhao X, Zhao Q. Effect of surface structure on photocatalytic activity of TiO<sub>2</sub> thin films prepared by sol-gel method. *Thin Solid Films.* 2000;379(1-2):7-14. [https://doi.org/10.1016/S0040-6090\(00\)01542-X](https://doi.org/10.1016/S0040-6090(00)01542-X)
54. Cardona M, Harbeke G. Optical properties and band structure of wurtzite-type crystals and rutile. *Phys Rev.* 1965;137(5A):A1467. <https://doi.org/10.1103/PhysRev.137.A1467>
55. Guz R, Moura C, Cunha MAA, Rodrigues MB. Factorial design application in photocatalytic wastewater degradation from TNT industry—red water. *Environ Sci Pollut Res.* 2017;24(7):6055-60. <https://doi.org/10.1007/s11356-016-6460-4>
56. Shyniya CR, Bhabu KA, Rajasekaran TR. Enhanced electrochemical behavior of novel acceptor doped titanium dioxide catalysts for photocatalytic applications. *J Mater Sci: Mater Electron.* 2017;28(9):6959-70. <https://doi.org/10.1007/s10854-017-6396-6>
57. Ge S, Xu H, Wang W, Cao R, Wu Y, Xu W, et al. The improvement of open circuit voltage by the sputtered TiO<sub>2</sub> layer for efficient perovskite solar cell. *Vacuum.* 2016;128:91-8. <https://doi.org/10.1016/j.vacuum.2016.03.013>
58. Schneider J, Matsuoka M, Takeuchi M, Zhang J, Horiuchi Y, Anpo M, et al. Understanding TiO<sub>2</sub> photocatalysis: mechanisms and materials. *Chem Rev.* 2014;114(19):9919-86. <https://doi.org/10.1021/cr5001892>
59. Bai J, Zhou B. Titanium dioxide nanomaterials for sensor applications. *Chem Rev.* 2014;114(19):10131-76. <https://doi.org/10.1021/cr400625j>
60. Mills A, Davies RH, Worsley D. Water purification by semiconductor photocatalysis. *Chem Soc Rev.* 1993;22:417-25. <https://doi.org/10.1039/CS9932200417>
61. Singh J, Sahu K, Pandey A, Kumar M, Ghosh T, Satpati B, et al. Atom beam sputtered Ag-TiO<sub>2</sub> plasmonic nanocomposite thin films for photocatalytic applications. *Appl Surf Sci.* 2017;411:347-54. <https://doi.org/10.1016/j.apsusc.2017.03.152>
62. Ogawa H, Higuchi T, Nakamura A, Tokita S, Miyazaki D, Hattori T, et al. Growth of TiO<sub>2</sub> thin film by reactive RF magnetron sputtering using oxygen radical. *J Alloys Compd.* 2008;499(1-2):375-8. <https://doi.org/10.1016/j.jallcom.2006.02.103>
63. Abeledo-Lameiro MJ, Reboledo-Fernández A, Polo-López MI, Fernández-Ibáñez P, Ares-Mazás E, Gómez-Couso H. Photocatalytic inactivation of the waterborne protozoan parasite *Cryptosporidium parvum* using TiO<sub>2</sub>/H<sub>2</sub>O<sub>2</sub> under simulated and natural solar conditions. *Catal Today.* 2017;280(1):132-8. <https://doi.org/10.1016/j.cattod.2016.05.046>
64. Podporska-Carroll J, Panaitescu E, Quilty B, Wang L, Menon L, Pillai SC. Antimicrobial properties of highly efficient photocatalytic TiO<sub>2</sub> nanotubes. *Appl Catal B Environ.* 2015;176-177:70-5. <https://doi.org/10.1016/j.apcatb.2015.03.029>
65. Guillén C, Montero J, Herrero J. Anatase and rutile TiO<sub>2</sub> thin films prepared by reactive DC sputtering at high deposition rates on glass and flexible polyimide substrates. *J Mater Sci.* 2014;49(14):5035-42. <https://doi.org/10.1007/s10853-014-8209-0>
66. Aguas Y, Hincapié M, Fernández-Ibáñez P, Polo-López MI. Solar photocatalytic disinfection of agricultural pathogenic fungi (*Curvularia* sp.) in real urban wastewater. *Sci Total Environ.* 2017;607-608:1213-24. <https://doi.org/10.1016/j.scitotenv.2017.07.085>
67. Singh J, Satpati B, Mohapatra S. Structural, optical and plasmonic properties of Ag-TiO<sub>2</sub> hybrid plasmonic nanostructures with enhanced photocatalytic activity. *Plasmonics.* 2017;12(3):877-88. <https://doi.org/10.1007/s11468-016-0339-6>
68. Wang L, Liu S, Wang Z, Zhou Y, Qin Y, Wang ZL. Piezotronic effect enhanced photocatalysis in strained anisotropic ZnO/TiO<sub>2</sub> nanoplatelets via thermal stress. *ACS Nano* 2016;10(2):2636-43. <https://doi.org/10.1021/acsnano.5b07678>
69. Méndez-Medrano MG, Kowalska E, Lehoux A, Herissan A, Ohtani B, Bahena D, et al. Surface modification of TiO<sub>2</sub> with Ag nanoparticles and CuO nanoclusters for application in photocatalysis. *J Phys Chem C.* 2016;120(9):5143-54. <https://doi.org/10.1021/acs.jpcc.5b10703>
70. Fechine GJM, Christensen PA, Egerton TA, White JR. Evaluation of poly(ethylene terephthalate) photostabilisation using FTIR spectrometry of evolved carbon dioxide. *Polym Degrad Stab.* 2009;94(2):234-9. <https://doi.org/10.1016/j.polymdegradstab.2008.10.025>
71. Fechine GJM, Rabello MS, Souto-Maior RM. The effect of ultraviolet stabilizers on the photodegradation of poly(ethylene terephthalate). *Polym Degrad Stab.* 2002;75(1):153-9. [https://doi.org/10.1016/S0141-3910\(01\)00214-2](https://doi.org/10.1016/S0141-3910(01)00214-2)
72. Fechine GJM, Rabello MS, Souto-Maior RM, Catalani LH. Surface characterization of photodegraded poly(ethylene terephthalate). The effect of ultraviolet absorbers. *Polymer.* 2004;45(7):2303-8. <https://doi.org/10.1016/j.polymer.2004.02.003>